Effect of Diffusional Limitations on Lineweaver-Burk Plots for Immobilized Enzymes

Lineweaver-Burk plots of reaction rate data obtained with immobilized enzymes need not be linear even when intrinsic enzyme kinetics follow the simple Michaelis-Menten rate expression. Theoretical calculations show that mass transfer effects may cause curvature which is concave or convex to the abscissa, depending upon experimental conditions. Consequently, graphical procedures commonly employed for analysis of soluble enzyme kinetics may yield misleading results when applied to immobilized enzymes. Three approaches which follow from the behavior of numerical and asymptotic solutions to the problem are proposed for extraction of intrinsic kinetic information.

BRUCE K. HAMILTON
COLIN R. GARDNER
and
CLARK K. COLTON

Department of Chemical Engineering
Massachusetts Institute of Technology
Cambridge, Massachusetts 02139

SCOPE

Practical application of enzymatic catalysis often requires that enzymes be immobilized, thereby permitting recovery and continuous use. It is important that the kinetics of immobilized enzymes be well understood to facilitate their economic utilization. In particular, it is necessary to account for the effect of diffusional limitations and to develop procedures which permit extraction of intrinsic kinetic parameters from observed reaction rates.

Native enzymes in solution typically follow hyperbolic Michaelis-Menten kinetics, Equation (1), which are formally analogous to Langmuir-Hinshelwood kinetics in heterogeneous catalysis. Graphical analysis of kinetic data is commonly carried out on transformed coordinates such as a Lineweaver-Burk plot of reciprocal reaction rate versus reciprocal substrate concentration. This serves to linearize the data so that the maximum reaction rate and the Michaelis constant can be evaluated directly from the intercept and slope. The same approach is often used with immobilized enzymes, but little attention has been paid to the precise physical meaning of the parameters so determined. Nonlinear Lineweaver-Burk plots have been reported in several experimental studies with enzymes immobilized in porous supports (Lilly and Sharp, 1968; Kay and Lilly, 1970; Bunting and Laidler, 1972); in all cases, the enzymes in solution gave Michaelis-Menten kinetics. It is unclear whether the curvature observed with immobilized enzymes stems from diffusional limitations, from changes in intrinsic enzyme kinetics after immobilization, or from other factors.

In this paper we examine through theoretical analysis the effect of diffusional limitations on the observed kinetics of immobilized enzymes. Of particular interest is the behavior of Lineweaver-Burk plots and the extraction of intrinsic kinetic parameters when diffusional effects are large. The problem considered is substrate diffusion in a homogeneous porous support in the form of a one-dimensional slab or membrane in which an enzyme that catalyzes a reaction following irreversible Michaelis-Menten kinetics is uniformly immobilized. Both internal and external diffusional resistances are considered, and emphasis is placed upon the asymptotic solution which is valid when diffusional effects are important and the modified Thiele modulus is large.

CONCLUSIONS AND SIGNIFICANCE

Lineweaver-Burk plots are calculated from the theoretical analysis for several specific examples, and the results are then generalized on dimensionless coordinates (Figures 4 and 5). Nonlinear behavior can occur when diffusional limitations are significant, and the shape of the curve depends upon the value of the Thiele modulus and the ratio of the Michaelis constant to the surface substrate concentration. At relatively low substrate concentrations, the Lineweaver-Burk plot is asymptotic to a straight line, the slope of which is much steeper than that obtained in the absence of diffusional influences. With increasing substrate concentration, the plot becomes concave with respect to the abscissa because of the influence of diffusion on the zero-order character of Michaelis-Menten kinetics, and the range of substrate concentrations over which this curvature is apparent increases with increasing Thiele modulus. At very high substrate concentration, the curve becomes convex because the effectiveness factor approaches unity and the plot becomes asymptotic to the straight line corresponding to diffusion-free kinetics. The presence of an external diffusion resistance diminishes the concave curvature and increases the slope of the plot. These results indicate that considerable caution should be exercised in the use of Lineweaver-Burk plots with immobilized enzymes because indiscriminate use may lead to kinetic parameter estimates which have little or no

Correspondence concerning this paper should be addressed to C. K. Colton. C. R. Gardner is with the Department of Chemistry, University of Aberdeen, Aberdeen, Scotland.

physical significance.

Three approaches are proposed for determination of intrinsic kinetic parameters when diffusion effects are large and their relative merits are compared. All three require only reaction rate measurements made as a function of either surface or bulk substrate concentration and are thus particularly valuable when variation of support thickness is not feasible.

We consider a porous matrix in the form of a one-dimensional slab or membrane of thickness L in which enzymatic activity is uniformly distributed. The intrinsic kinetics of the immobilized enzyme are assumed to follow the irreversible Michaelis-Menten expression

$$v = \frac{V_m s}{K_m + s} \tag{1}$$

One surface of the membrane is impermeable to substrate and the other is maintained at a uniform concentration s_s. It is assumed that substrate diffusion within the membrane can be represented by Fick's first law with a concentration-independent effective diffusivity D_{eff}, that there are no interactions between the substrate and the porous support, and that V_m and K_m are the same for all immobilized enzyme. At steady state, a substrate mass balance over a differential volume element yields in dimensionless form

$$\frac{d^2\sigma}{dz^2} - \phi_m^2 \nu \left(\frac{\sigma}{\nu + \sigma}\right) = 0 \tag{2}$$

where $\sigma = s/s_s$ is a dimensionless substrate concentration, $z = x/L$ is a dimensionless distance, $\nu = K_m/s_s$ is a dimensionless Michaelis constant, and the modified Thiele modulus is defined by

$$\phi_m = L\left[\frac{V_m}{K_m D_{\text{eff}}}\right]^{1/2} \tag{3}$$

The boundary conditions are

$$\text{I.} \qquad \sigma = 1 \text{ at } z = 0 \tag{4}$$

$$\text{II.} \qquad \frac{d\sigma}{dz} = 0 \text{ at } z = 1 \tag{5}$$

SOLUTIONS FOR EFFECTIVENESS FACTOR

The effectiveness factor η is defined as the observed rate of reaction in the membrane divided by that which would obtain if the substrate concentration was uniformly equal to its value at the surface:

$$v_{\text{obs}} = \eta \frac{V_m s_s}{K_m + s_s} \tag{6}$$

η is a function of ϕ_m and ν.

A problem equivalent to the one of interest here but cast in terms of analogous Langmuir-Hinshelwood kinetics was first treated numerically by Prater and Lago (1956) and by Chu and Hougen (1962), and subsequently in more general fashion by Roberts and Satterfield (1965), Krasuk and Smith (1965), and Schneider and Mitschka (1965). Atkinson and Daoud (1968) fitted these numerical results with high accuracy to a single empirical function by use of a least squares procedure. Related work dealing with more complex kinetic schemes and other geometries has been reviewed (Satterfield, 1970; Aris, 1974). We have employed the numerical procedure of Roberts (1965) which involves selection of a value for σ at $z = 1$ followed by a marching finite-difference integration to solve for s_s and η.

An approximate analytical solution is obtained if boundary condition II is replaced by

$$\text{IIa.} \qquad \sigma = 0 \text{ at } z = 1 \tag{7}$$

This corresponds to the case of large ϕ_m where reaction is very rapid relative to diffusion and substrate does not penetrate far into the porous matrix. This notion was first employed by Zeldovich, as cited by Frank-Kamenetskii (1955), and has been discussed in depth by Bischoff (1965) and Petersen (1965). The solution for effectiveness factor (Roberts and Satterfield, 1965; Bischoff, 1965) is given by

$$\eta \simeq \tilde{\eta} = \frac{\sqrt{2}}{\phi_m}(1 + \nu)[\nu^{-1} - \ln(1 + \nu^{-1})]^{1/2} \tag{8}$$

where superscript tilde denotes that the solution is obtained with boundary condition IIa. Figure 1 shows the region of the $\phi_m - \nu$ plane within which the asymptotic and numerical solutions agree to within 1%. Also plotted vs. ν are the values of η along the border of that region.

The asymptotic behavior of η led Bischoff (1965) to suggest use of a general modulus

$$m = \frac{1}{\tilde{\eta}} \tag{9}$$

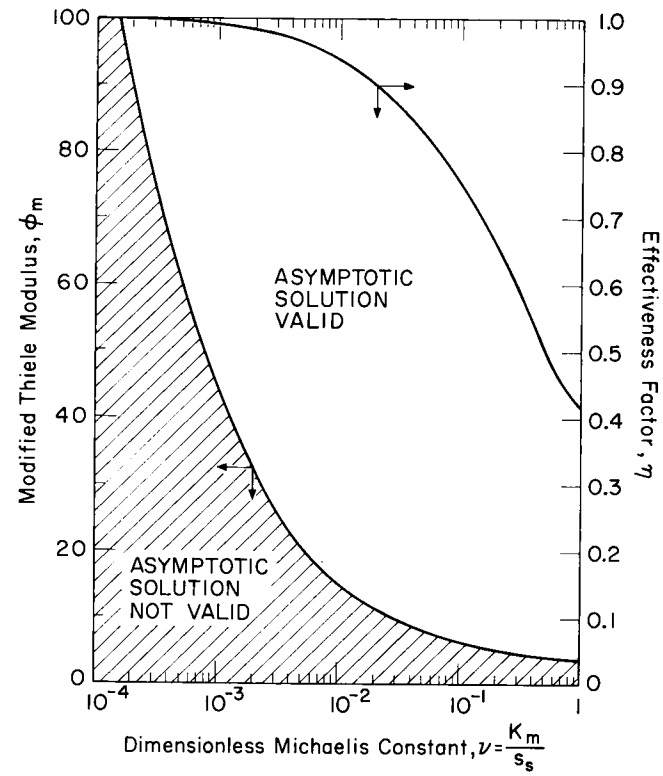

Fig. 1. Values of ϕ_m and ν above which asymptotic solution, Equation (8), agrees with numerical solution to within 1%. As $\nu \to \infty$, Equation (8) valid for $\phi_m > 3$. η corresponding to limits of validity is plotted versus ν.

which permits compact graphical representation of the results because solutions for η have common asymptotes (for all ν) at high and low values of m. This approach has been followed by Moo-Young and Kobayashi (1972) in an analysis which included various kinetic expressions typical of enzymatic reactions. For the present problem, they suggested the following empirical approximation in terms of the general modulus m:

$$\eta \simeq \frac{\eta_0' + \nu\eta_1'}{1+\nu} \tag{10}$$

where

$$\eta_0' = \begin{cases} 1 \ (0 < m \leq 1) \\ \dfrac{1}{m} \ (m > 1) \end{cases} \tag{11}$$

$$\eta_1' = \frac{\tanh m}{m} \tag{12}$$

The largest deviation between η calculated from Equation (10) and from the numerical solution was found to be 0.089 at $m = 1$, and $\nu = 0.2$. Kobayashi and Laidler (1973) subsequently employed Equation (10) in developing several approximate procedures for evaluating intrinsic kinetic parameters. Horvath and Engasser (1973) used the general modulus in treating irreversible Michaelis-Menten kinetics in spheres and spherical shells. Fink et al. (1973) have analyzed the same problem for slabs, cylinders, and spheres in the presence of external mass transfer resistances but with a different modulus. We have retained the use of ϕ_m and ν because they permit separation of concentration- and nonconcentration-dependent parameters; the same approach was taken recently by Thomas et al. (1972) and by Marsh et al. (1973).

The limiting behavior of $\tilde{\eta}$ when ν^{-1} (the dimensionless surface substrate concentration) is large or small will be of subsequent interest. When ν^{-1} is small compared to unity, one finds by expansion of Equation (8):

$$\tilde{\eta} \simeq \frac{1 + \frac{2}{3}\nu^{-1} + 0(\nu^{-2})}{\phi_m} \tag{13}$$

so that the asymptotic expression for a first-order reaction is recovered in the limit

$$\lim_{\nu^{-1}\to 0} \tilde{\eta} = \lim_{\phi_m \to \infty} \eta_1 = \frac{1}{\phi_m} \tag{14}$$

where the first-order rate constant is given by V_m/K_m. Conversely, when ν^{-1} is much greater than unity, $\tilde{\eta}$ is given approximately by the expression for a zero-order reaction

$$(\nu^{-1} >> 1) \quad \tilde{\eta} \simeq \eta_0 = \frac{\sqrt{2}}{\phi_m \nu^{1/2}} \tag{15}$$

which is valid for $\phi_m\nu^{1/2} > \sqrt{2}$ ($\eta_0 = 1$ for $\phi_m\nu^{1/2} \leq \sqrt{2}$). While the zero- and first-order expressions have been used for convenience in several recent analyses (Van Duijn et al., 1967; Goldman et al., 1968; Sundaram et al., 1970; Rony, 1971; Kasche et al., 1971; Blaedel et al., 1972; Lasch, 1972; Vieth et al., 1973; Gondo et al., 1973), it will be seen that the use of the full expression for $\tilde{\eta}$, Equation (8), is more desirable than either of Equations (14) or (15).

LINEWEAVER-BURK PLOTS

Equation (6) can be rearranged into a form suitable for plotting on Lineweaver-Burk coordinates of reciprocal observed reaction rate vs. reciprocal surface concentration:

$$\frac{1}{v_{obs}} = \frac{K_m}{\eta V_m}\frac{1}{s_s} + \frac{1}{\eta V_m} = \frac{1+\nu}{\eta V_m} \tag{16}$$

We first consider cases for which the asymptotic solution $\eta \simeq \tilde{\eta}$ is valid. A combination of Equations (8) and (16) yields

$$\frac{1}{\tilde{v}_{obs}} = \frac{\phi_m}{\sqrt{2}\,V_m}\left[\nu^{-1} - \ln(1+\nu^{-1})\right]^{-1/2} \tag{17}$$

which is clearly nonlinear. The shape of the curve on Lineweaver-Burk coordinates can be ascertained by examination of the second derivative:

$$\frac{V_m}{\phi_m K_m^2}\frac{d^2(\tilde{v}_{obs}^{-1})}{d(s_s^{-1})^2} = \frac{1}{2\sqrt{2}}\Big\{\frac{3}{2}[\nu^{-1} - \ln(1+\nu^{-1})]^{-5/2}(\nu^3+\nu^2)^{-2} - [\nu^{-1} - \ln(1+\nu^{-1})]^{-3/2}\frac{(3\nu^2+2\nu)}{(\nu^3+\nu^2)^2}\Big\} \tag{18}$$

The right hand side of Equation (18) is always negative for all positive values of ν. Thus, a Lineweaver-Burk plot is always concave to the $1/s_s$ axis in the region where Equation (18) is valid. The magnitude of the curvature is dependent upon ν, ϕ_m, K_m, and V_m.

When ν^{-1} is small with respect to unity, Equations (13) and (16) may be combined to give

$$\frac{1}{\tilde{v}_{obs}} \simeq \frac{\phi_m}{V_m}\left(\nu + \frac{1}{3}\right) \tag{19}$$

which, on Lineweaver-Burk coordinates, is the equation for a straight line with a slope of $\phi_m K_m/V_m$ and extrapolated intercept on the ordinate of $\phi_m/3V_m$. If mass transfer effects were absent and Equation (1) were valid for v_{obs}, the slope would be K_m/V_m and the intercept $1/V_m$. With decreasing ν^{-1} the plot becomes indistinguishable from that expected for first-order kinetics at large ϕ_m:

$$\lim_{\nu^{-1}\to 0}\frac{1}{\tilde{v}_{obs}} = \frac{\phi_m}{V_m}\nu \tag{20}$$

wherein the slope remains the same as in Equation (19), but the intercept is now zero.

At the other extreme, when $\nu^{-1} >> 1$, Equations (15) and (16) provide the result expected for zero-order kinetics:

$$\frac{1}{\tilde{v}_{obs}} \simeq \frac{\phi_m}{\sqrt{2}\,V_m}\nu^{1/2} \tag{21}$$

In this region, the curvature of the Lineweaver-Burk plot reaches its maximum value:

$$\frac{V_m}{\phi_m K_m^2}\frac{d^2(\tilde{v}_{obs}^{-1})}{d(s_s^{-1})^2} \simeq -\frac{\nu^{-3/2}}{4\sqrt{2}} \tag{22}$$

We therefore conclude that the expected concave curvature of a Lineweaver-Burk plot for immobilized enzymes is associated with the influence of diffusional limitations on the zero-order character of Michaelis-Menten kinetics.

The slope at any point on a Lineweaver-Burk plot with η less than unity is greater than that in the complete ab-

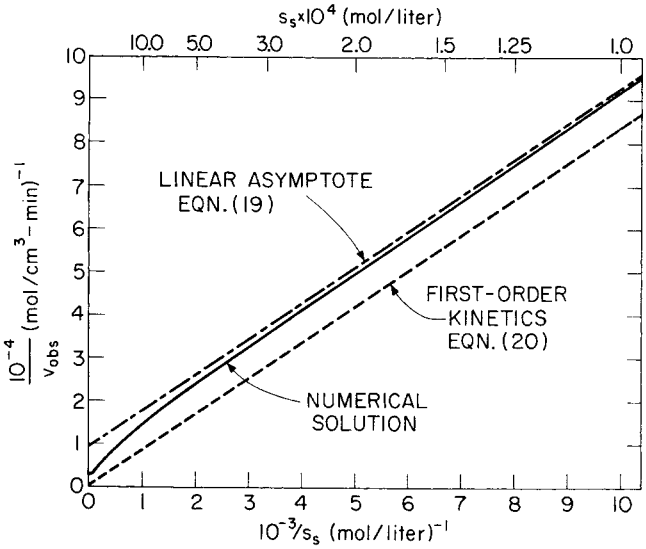

Fig. 2. Lineweaver-Burk plot calculated with parameters in Table 1. Maximum $\nu \simeq 3$.

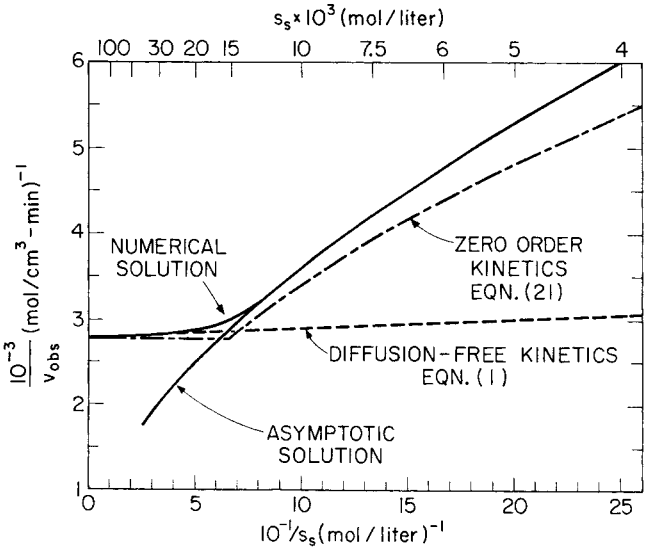

Fig. 3. Expanded plot of lower left-hand corner of Figure 2. Maximum $\nu \simeq 0.075$.

sence of mass transfer effects, as shown by comparison of Equations (1) and (16). As ν^{-1} increases at constant ϕ_m, a region must be reached where Equation (8) no longer holds, the effectiveness factor approaches unity, and the curve becomes asymptotic to the line which corresponds to Equation (1). It follows that near $\nu = 0$ there must be a region in which the Lineweaver-Burk plot is convex to the $1/s_s$ axis.

Numerical Example

A specific numerical example is presented in Figures 2 and 3 which display all the characteristics that might be observed in a Lineweaver-Burk plot for an immobilized enzyme. The relevant parameters were chosen so as to be typical of a physically realizable system and are tabulated in Table 1. The results were generated using the numerical procedure of Roberts (1965) and the various analytical expressions described above.

Figure 2 covers a range of relatively low surface substrate concentrations (minimum 10^{-4} M, $\nu = 3$). Over virtually the entire range plotted, the numerical solution

Table 1. Parameter Values for Numerical Example

Parameter			Source
L	=	5.0×10^{-3} cm	
K_m	=	3.0×10^{-4} M	Barman, 1969*
n_0	=	2.07×10^{1} mol product/(mol enzyme-sec)	Lehninger, 1970*
M	=	6.5×10^{4} g/mol	Barman, 1969*
ρ_E	=	18.9×10^{-3} g enzyme/cm^3 support	Pitcher, 1973*
D_{eff}	=	5.0×10^{-6} cm^2/s	
V_m	=	$\frac{\rho_E n_0}{M} = 6.0 \times 10^{-6}$ mol product/(s-cm^3 support)	
ϕ_M	=	$L(V_m/K_m D_{eff})^{1/2} = 10.0$	

* Values of V_m and M are for α-phosphoglucomutase; K_m is for β-phosphoglucomutase; ρ_E is typical of currently attainable enzyme loading with porous glass supports.

and asymptotic solution coincide. Except near the origin, diffusion limitations are significant, and the effectiveness factor is much less than unity. In the upper right-hand corner, the curve converges asymptotically towards the line given by Equation (19), whereas agreement with the first-order approximation, Equation (20), is relatively poor. The curve is apparently linear and well-represented by Equation (19) for $\nu \gtrsim 1$. In the lower left-hand corner, the curve is clearly concave to the abscissa.

The lower left-hand corner of Figure 2 is shown with an expanded scale in Figure 3. The curve is predominantly concave towards the abscissa with an inflection point where the numerical solution and asymptotic analytical solution diverge. The remainder of the curve at higher substrate concentration is convex as it asymptotically approaches the straight line which corresponds to the absence of diffusion limitations. The curve corresponding to zero-order kinetics shows only fair agreement with the numerical solution in the lower left-hand corner of the plot.

Generalized Coordinates

Results of the numerical and asymptotic solutions are plotted on generalized Lineweaver-Burk coordinates, as suggested by the form of the asymptotic solution, in Figures 4 and 5. These plots show clearly the relationship between regions of the $\phi_m - \nu$ plane which have linear, concave, or convex character.

For $\phi_m \gtrsim 3$ and $\nu \gtrsim 1$, all plots lie on the asymptotic solution which is nearly linear. As ν decreases, the curve becomes increasingly concave with respect to the abscissa until a value of ν (shown in Figure 1) is reached where the true (numerical) solution peels off the asymptotic solution and the curve is convex. Maximum curvature, both concave and convex, is associated with large diffusional effects (large ϕ_m) and high surface substrate concentration (low ν).

With decreasing ϕ_m the curvature, first concave, then convex, disappears. For $\phi_m \lesssim 0.5$, $\eta \simeq 1.0$, and linear Michaelis-Menten behavior is obtained.

External Mass Transfer Resistance

To this point, the problem has been cast in terms of a known surface substrate concentration s_s. In many situations, this is not directly measurable because of partitioning and external mass transfer influences which can limit the observed rate of reaction (O'Neill, 1972).

We consider an external concentration boundary layer,

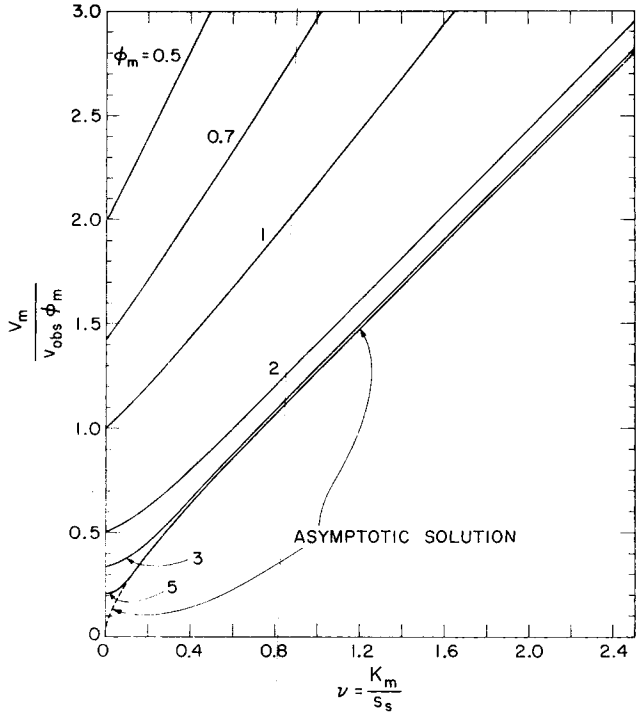

Fig. 4. Lineweaver-Burk plots on generalized dimensionless coordinates for $\phi_m \leq 5$.

but the analysis is easily generalized to include a semipermeable membrane. The steady state flux of substrate per unit area may be expressed by

$$J_s = k(s_b - s_i) \tag{23}$$

where the mass transfer coefficient k is assumed constant over the surface of the porous medium. The surface substrate concentration is related to s_i by

$$s_s = K_p\, s_i \tag{24}$$

where the partition coefficient K_p is the equilibrium ratio at the membrane-solution interface of the substrate concentration within the membrane voids divided by the concentration in the external solution. Substrate flux is also given by

$$J_s = v_{obs}\, L \tag{25}$$

Combination of Equations (23) through (25) leads to

$$s_b = \frac{s_s}{K_p} + \frac{v_{obs}\, L}{k} \tag{26}$$

Equation (26) can be used with the relations developed above to calculate Lineweaver-Burk plots in terms of the measurable concentration s_b.

Figure 6 presents numerical examples of Lineweaver-Burk plots calculated for a wide range of mass transfer coefficients with all other parameters the same as those listed in Table 1 and with $K_p = 1.0$. The curves are plotted over the region where the asymptotic analytical solution is valid, and therefore the curve for infinite mass transfer coefficient is concave to the abscissa. As the external mass transfer resistance increases, the curvature decreases, and the curve for the lowest mass transfer coefficient is virtually linear. The curves have a qualitative similarity to the experimental observations reported in Figure 9 of Lilly and Sharp (1968) where decreasing agitation rate produced a more linear Lineweaver-Burk plot.

DETERMINATION OF INTRINSIC KINETIC PARAMETERS

The preceding results can be applied to evaluation of the intrinsic kinetic parameters V_m and K_m. We assume that the intrinsic kinetics of all the immobilized enzyme follow the form of the irreversible Michaelis-Menten rate law with the same values of V_m and K_m; that D_{eff} and K_p can be measured independently by using established procedures (Colton et al., 1971; Satterfield et al., 1973) under conditions such that the immobilized enzyme is inactivated or an essential cofactor is absent from the solution; and that experiments can be carried out in a

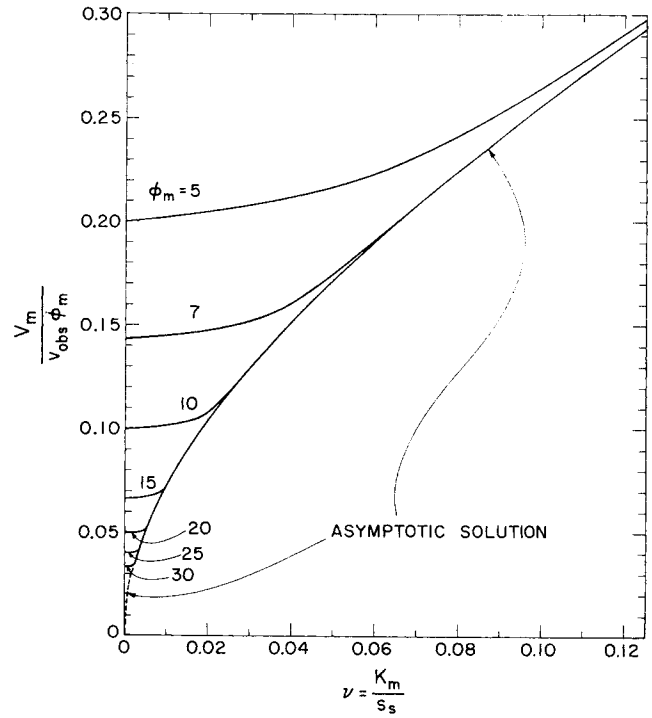

Fig. 5. Expanded plot of lower left-hand corner of Figure 4 for $\phi_m \geq 5$.

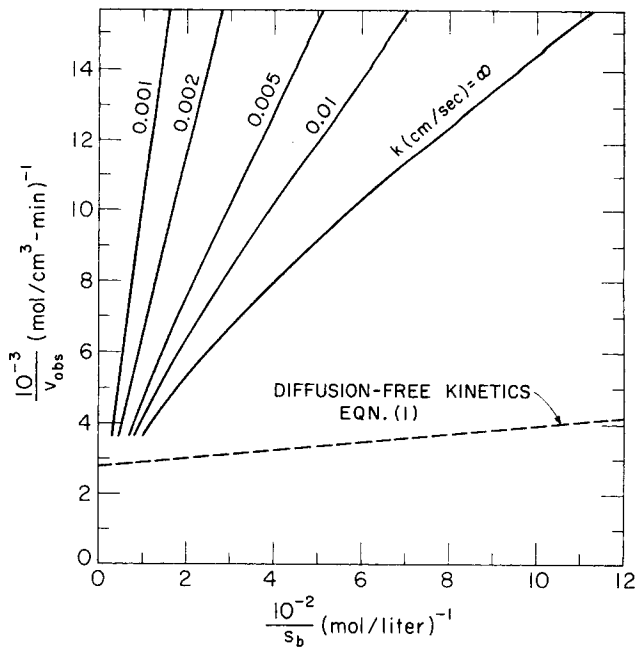

Fig. 6. Effect of external mass transfer resistance of Lineweaver-Burk plots calculated with parameters in Table 1.

manner such that external mass transfer resistances are negligible or that they can be evaluated by standard techniques (Rovito and Kittrell, 1973; Satterfield, 1970), thereby permitting calculation of s_s from known s_b by use of Equations (23) and (24).

We discuss three straightforward approaches, which involve no approximations, for evaluation of V_m and K_m from initial rate measurements when diffusional effects are significant. All follow directly from the previous developments. Where these approaches are limited by applicability of the asymptotic solution, it is useful for the experimentalist to have a criterion of validity which contains only quantities that can be either measured directly or predicted. Such a criterion is provided by the dimensionless modulus (Wagner, 1943)

$$\Phi_L = \frac{L^2 v_{obs}}{D_{eff} s_s} \tag{27}$$

which, for Michaelis-Menten kinetics, is also given by (Roberts and Satterfield, 1965)

$$\Phi_L = \frac{\eta \phi_m^2}{1 + \nu^{-1}} \tag{28}$$

By use of the results in Figure 1 and Equation (28), the criterion for validity of the asymptotic solution is found to be $\Phi_L \gtrsim 3$.

1. *Lineweaver-Burk Plot.* In view of the curvature displayed by Lineweaver-Burk plots with immobilized enzymes when mass transfer effects are significant, the rationale for their general use is questionable. However, when experimental conditions are such that the asymptotic solution is valid (Figure 1) and $\nu > 1$ ($\nu >> 1$ preferably), a nearly linear plot results (Figures 2 and 4) from which the slope and extrapolated intercept provide estimates of V_m and K_m. From Equation (19) one finds

$$\frac{\text{Slope}}{\text{Intercept}} = 3K_m \tag{29}$$

Substitution of K_m thus evaluated into Equation (19) or the expression for the slope or intercept yields an estimate of V_m.

It must be cautioned, however, that an apparently linear Lineweaver-Burk plot does not by itself justify use of this approach, particularly when the experiments are carried out over a relatively narrow range of bulk substrate concentrations. Radii of curvature, as shown by the examples in this study, are large, and therefore the nonlinearity may be obscured by moderate experimental scatter. The pervasiveness of external mass transfer limitations will also tend to linearize Lineweaver-Burk plots. As a final precaution, it is apparent from Figure 2 that the estimate of the intercept will in general be rather sensitive to imprecision in the data, and this can be expected to result in relatively large confidence intervals for the estimate of K_m and V_m.

2. *Asymptotic Solution.* Equation (17) may be written in the form

$$\tilde{v}_{obs} = \frac{\sqrt{2} V_m}{\phi_m} f(\nu^{-1}) \tag{30}$$

Measurements of reaction velocity at two surface substrate concentrations under conditions where the asymptotic solution is valid therefore provide a means for implicit evaluation of K_m (without prior knowledge of V_m) from

$$\frac{v_{obs,1}}{v_{obs,2}} = \frac{f(\nu_1^{-1})}{f(\nu_2^{-1})} \tag{31}$$

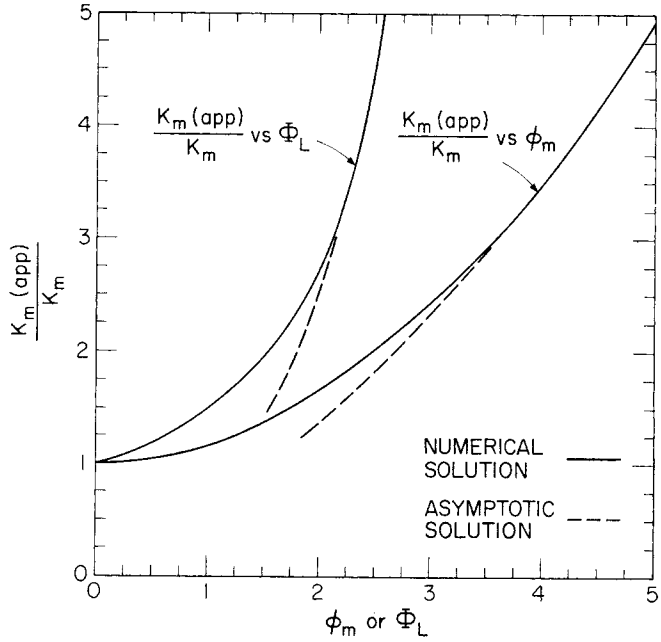

Fig. 7. Dependence of $K_m(app)/K_m$ on ϕ_m or Φ_L. $K_m(app)$ is defined as s_s at which $v_{obs} = V_m/2$. On this plot, $\Phi_L = L^2 V_m / 2 D_{eff} s_s$.

V_m can then be obtained explicitly from Equation (30).

Alternatively, if V_m is evaluated by independent means (see below), K_m may be obtained from a single measurement by implicit solution of Equation (30). The limitation of asymptotic solution validity can be circumvented through use of the empirical function of Atkinson and Daoud (1968), or, if moderate inaccuracy can be tolerated, Equation (10). In any event, the insensitivity of the ratio expressed by Equation (31) to substrate concentration makes difficult the precise evaluation of K_m by this approach from experiments for which $\nu << 1$.

3. *Apparent* K_m. A recent recommendation (Sundaram et al., 1972) suggests reporting data in terms of K_m(app) which is defined as the substrate concentration that gives a reaction velocity corresponding to one-half V_m(app). We assume here that V_m(app) is the same as V_m, an independent estimate of which must be obtained experimentally. Equation (6) then may be written as

$$\frac{v_{obs}}{V_m} = \frac{1}{2} = \frac{\eta}{1 + \dfrac{K_m}{K_m(app)}} \tag{32}$$

The value of ϕ_m for which Equation (32) is satisfied can be determined from the numerical and asymptotic solutions (for example, Figures 4 and 5) by substituting K_m/K_m(app) for ν. The results are shown in Figure 7. Given a measurement of K_m(app), Figure 7 may be used to find the value of K_m which places the calculated K_m(app)$/K_m$ and ϕ_m on the curve (or by implicit evaluation of the asymptotic solution where applicable).

Figure 7 also presents a plot of K_m(app)$/K_m$ as a function of Φ_L. The latter was calculated from Equation (28) with ν^{-1} replaced by K_m(app)$/K_m$, with $v_{obs} = V_m/2$, and with the corresponding values of η and ϕ_m. This curve permits direct evaluation of K_m from a measurement of K_m(app) without need for iterative calculations.

In principle, V_m may be estimated by making reaction rate measurements over a range of relatively high substrate concentrations (provided substrate inhibition is absent) and extrapolating to infinite substrate concentration

on Lineweaver-Burk coordinates. However, this procedure presents difficulties when ϕ_m is large. Figure 5 shows the abrupt change in slope which occurs in the shift from concave to convex curvature. Clearly, accurate evaluation of V_m requires that measurements be made in the convex portion of the curve, that is, very low values of ν in the region where the asymptotic solution is not valid. Substrate solubility may limit the extent to which this requirement can be achieved.

ACKNOWLEDGMENTS

This work was supported in part by National Science Foundation Grant GI 34284 and by a grant from the Camille and Henry Dreyfus Foundation. Suggestions by Dr. Malcolm K. Lilly, University College, London, and Professor Charles N. Satterfield, M.I.T., are gratefully acknowledged.

NOTATION

D_{eff} = effective substrate diffusivity in porous matrix, cm²/s
J_s = substrate flux per unit external surface area of support, mol/cm²-s
K_m = Michaelis constant, mol/liter
K_m(app) = apparent Michaelis constant, equal to s_s when $v_{obs} = V_m/2$
K_p = partition coefficient, equal to s_s/s_i at equilibrium
k = interphase mass transfer coefficient, cm/s
L = slab or membrane thickness, cm
M = enzyme molecular weight, g/mol
m = dimensionless general modulus, defined by Equation (9)
n_0 = enzyme turnover number, mol product/mol enzyme-s
s = substrate concentration, mol/liter
s_b = bulk substrate concentration, mol/liter
s_i = substrate concentration in external solution at interface, mol/liter
s_s = substrate concentration in membrane voids at interface, mol/liter
V_m = maximum reaction velocity at enzyme saturation, $\rho_E n_0/M$, mol product/cm³-s
v = reaction velocity, mol product/cm³-s
v_{obs} = observed reaction velocity, mol product/cm³-s
$\tilde{v}_{obs}$ = observed reaction velocity predicted by asymptotic expression, Equation (17)
x = longitudinal distance from membrane surface, cm
z = dimensionless distance, x/L

Greek Letters

η = effectiveness factor (dimensionless)
η_0 = effectiveness factor for zero-order kinetics
η_1 = effective factor for first order kinetics
η_0' = parameter defined by Equation (11)
η_1' = parameter defined by Equation (12)
$\tilde{\eta}$ = effectiveness factor predicted by asymptotic expression, Equation (8)
ν = dimensionless Michaelis constant, K_m/s_s
ρ_E = volumetric density of immobilized enzyme, g enzyme/cm³
σ = dimensionless substrate concentration, s/s_s porous support
Φ_L = dimensionless modulus, defined by Equation (27)
ϕ_m = modified dimensionless Thiele modulus $L[V_m/K_m D_{eff}]^{1/2}$

LITERATURE CITED

Aris, R., *The Mathematical Theory of Diffusion and Reaction in Permeable Catalysts,* Oxford at Clarendon Press, London (1974).

Atkinson, B., and S. Daoud, "The Analogy Between Microbiological 'Reactions' and Heterogeneous Catalysis," *Trans. Instn. Chem. Engrs.*, **46**, T19 (1968).

Barman, T. E., *Enzyme Handbook,* Springer-Verlag, New York (1969).

Bischoff, K. B., "Effectiveness Factors for General Reaction Rate Forms," *AIChE J.*, **11**, 351 (1965).

Blaedel, W. J., T. R. Kissel, and R. C. Boguslaski, "Kinetic Behavior of Enzymes Immobilized in Artificial Membranes," *Anal. Chem.*, **44**, 2030 (1972).

Bunting, P. S., and K. J. Laidler, "Kinetic Studies on Solid-Supported β-Galactosidase," *Biochem.*, **11**, 4477 (1972).

Chu, C., and O. A. Hougen, "The Effect of Adsorption on the Effectiveness Factor of Catalyst Pellets," *Chem. Eng. Sci.*, **17**, 167 (1962).

Colton, C. K., K. A. Smith, E. W. Merrill, and P. C. Farrell, "Permeability Studies with Cellulosic Membranes," *J. Biomed. Mater. Res.*, **5**, 459 (1971).

Fink, D. J., T. Na, and J. S. Schultz, "Effectiveness Factor Calculations for Immobilized Enzyme Reactions," *Biotech. Bioeng.*, **15**, 879 (1973).

Frank-Kamenetskii, D. A., *Diffusion and Heat Exchange in Chemical Kinetics,* N. Thon, (transl.), Princeton Univ. Press, New Jersey (1955).

Goldman, R., O. Kedem, and E. Katchalski, "Papain-Collodion Membranes. II. Analysis of the Kinetic Behavior of Enzymes Immobilized in Artificial Membranes," *Biochem.*, **7**, 4518 (1968).

Gondo, S., T. Sato, and K. Kusunoki, "Note on the Lineweaver-Burk Plots for the Immobilized Enzyme Particle," *Chem. Eng. Sci.*, **28**, 1773 (1973).

Horvath, C., and J. M. Engasser, "Pellicular Heterogeneous Catalysts. A Theoretical Study of the Advantages of Shell Structured Immobilized Enzyme Particles," *Ind. Eng. Chem. Fundamentals*, **12**, 229 (1973).

Kasche, V., H. Lundqvist, R. Bergman, and R. Axén, "A Theoretical Model Describing Steady-State Catalysis by Enzymes Immobilized in Spherical Gel Particles. Experimental Study of α-Chymotrypsin-Sepharose," *Biochem. Biophys. Res. Commun.*, **45**, 615 (1971).

Kay, G., and M. D. Lilly, "The Chemical Attachment of Chymotrypsin to Water-Insoluble Polymers Using 2-Amino-4,6-dichloro-5-triazine," *Biochem. Biophys. Acta*, **198**, 276 (1970).

Kobayashi, T., G. Van Dedem, and M. Moo-Young, "Oxygen Transfer into Mycelial Pellets," *Biotech. Bioeng.*, **15**, 27 (1973).

Kobayashi, T., and K. J. Laidler, "Kinetic Analysis for Solid-Supported Enzymes," *Biochem. Biophys. Acta*, **302**, 1 (1973).

Krasuk, J. H., and J. M. Smith, "Effectiveness Factors with Surface Diffusion," *Ind. Eng. Chem. Fundamentals*, **4**, 102 (1965).

Lasch, J., "Theoretical Analysis of the Kinetics of Enzymes Immobilized in Spherical Pellets," in *Analysis and Simulation of Biochemical Systems,* p. 295, H. C. Henker and B. Hess (eds.), American Elsevier, New York (1972).

Lehninger, A. L., *Biochemistry,* Worth, New York (1970).

Lilly, M. D., and A. K. Sharp, "The Kinetics of Enzymes Attached to Water-Insoluble Polymers," *Chemical Engineer*, CE12 (1968).

Marsh, D. R., Y. Y. Lee, and G. T. Tsao, "Immobilized Glucoamylase on Porous Glass," *Biotech. Bioeng.*, **15**, 483 (1973).

Moo-Young, M., and T. Kobayashi, "Effectiveness Factors for Immobilized-Enzyme Reactions," *Can. J. Chem. Eng.*, **50**, 162 (1972).

O'Neill, S. P., "External Diffusional Resistance in Immobilized Enzyme Catalysis," *Biotech. Bioeng.*, **14**, 675 (1972).

Petersen, E. E., *Chemical Reaction Analysis,* Prentice-Hall, Englewood Cliffs, N. J. (1965).

Pitcher, W. H., Corning Glass Works, New York, private communication (1973).

Prater, C. D., and R. M. Lago, "The Kinetics of the Cracking

of Cumene by Silica-Alumina Catalysts," in *Adv. Cat.* W. G. Frandenburg and V. I. Komarensky (eds.), 8, Academic Press, New York (1956).
Roberts, G. W., "I. Kinetics of Thiophene Hydrogenolysis. II. Effectiveness Factors for Porous Catalysts," Sc.D. thesis, Mass. Inst. of Technology, Cambridge (1965).
———., and C. N. Satterfield, "Effectiveness Factor for Porous Catalysts," *Ind. Eng. Chem. Fundamentals*, 4, 289 (1965).
Rony, P. R., "Multiphase Catalysis. II. Hollow Fiber Catalysts," *Biotech. Bioeng.*, 13, 431 (1971).
Rovito, B. J., and J. R. Kittrell, "Film and Pore Diffusion Studies with Immobilized Glucose Oxidase," *ibid.*, 15, 143 (1973).
Satterfield, C. N., *Mass Transfer in Heterogeneous Catalysis*, MIT Press, Cambridge (1970).
———., C. K. Colton, and W. H. Pitcher, Jr., "Restricted Diffusion in Liquids within Fine Pores," *AIChE J.*, 19, 628 (1973).
Schneider, P., and P. Mitschka, "Effect of Internal Diffusion on Catalytic Reaction," *Collection Czechoslov. Chem. Commun.*, 30, 146 (1965).
Sundaram, P. V., A. Tweedale, and K. J. Laidler, "Kinetic Laws for Solid-Supported Enzymes," *Can. J. Chem.*, 48, 1498 (1970).
Sundaram, P. V., E. K. Pye, T. M. S. Chang, V. H. Edwards, E. A. Humphrey, N. O. Kaplan, E. Katchalski, Y. Levin, M. D. Lilly, G. Manecke, K. Mosback, A. Patchornik, J. Porath, H. H. Weetall, and L. B. Wingard, Jr., "Recommendations for Standardization of Nomenclature in Enzyme Technology," p. 15, *Enzyme Eng.*, L. B. Wingard, Jr. (ed.), Interscience, N. Y. (1972).
Thomas, D., G. Broun, and E. Selegny, "Monoenzymatic Model Membranes: Diffusion-Reaction Kinetics and Phenomena," *Biochim.*, 54, 229 (1972).
Van Duijn, P., E. Pascoe, and M. Van der Ploeg, "Theoretical and Experimental Aspects of Enzyme Determination in a Cytochemical Model System of Polyacrylamide Films Containing Alkaline Phosphatase," *J. Hist. Cytochem.*, 15, 631 (1967).
Vieth, W. R., A. K. Mendiratta, A. O. Mogensen, R. Saini, and K. Venkatasubramanian, "Mass Transfer and Biochemical Reaction in Enzyme Membrane Reactor Systems. I. Single Enzyme Reactions," *Chem. Eng. Sci.*, 28, 1013 (1973.)
Wagner, C., "Über das Zusammenwinker von Strömung, Diffusion und chemischer Reaktion bei der heterogenen Katalyse," *Z. Phys. Chem.*, 193, 1 (1943).

Manuscript received October 19, 1973; revision received January 21 and accepted January 22, 1974.

Effect of Phase-Volume Ratio and Phase-Inversion on Viscosity of Microemulsions and Liquid Crystals

Microemulsions, which are optically transparent oil-water dispersions, were spontaneously produced upon mixing hexadecane, hexanol, potassium oleate, and water in specific proportions. The viscosity of the microemulsions was measured for several water/oil ratios including the phase-inversion region. The striking optical and viscosity changes observed at specific water/oil ratios were in agreement with the proposed mechanism of phase-inversion, namely, water spheres → water cylinders → water lammellae → continuous water phase, for this system. In the phase-inversion region, the dispersion exhibited birefringence and rheopectic properties. An extremely high viscosity (> 100,000 cps) exhibited by the dispersions between water/oil ratios of 2.0 and 3.5 were explained in terms of ion-dipole association between oleate and hexanol molecules on adjacent droplets.

J. W. FALCO
R. D. WALKER, JR.
and
D. O. SHAH

Departments of Chemical Engineering and Anesthesiology
University of Florida
Gainesville, Florida 32611

SCOPE

Microemulsions which are optically transparent isotropic oil-water dispersions can be formed spontaneously by using a combination of emulsifiers. Such oil-in-water or water-in-oil microemulsions consist of droplets 100-600 A in diameter. The objectives of the present study were to elucidate the effect of oil/water ratio and phase-inversion phenomenon on the viscosity of these dispersions and to correlate the changes in viscosity with the structural changes in the dispersions.

Since microemulsions form spontaneously and exhibit low viscosity, they have been considered promising for secondary and tertiary recovery in oil-fields (Gogarty and Tosch, 1968; Hill et al., 1973; Pursley et al., 1973). The phase-inversion region exhibits birefringence indicating structural anisotropy of the system. Previous studies from this laboratory have established that the phase-inversion region consists of liquid-crystalline structures. The rheological properties of microemulsions and liquid-crystalline systems are of considerable interest to investigators in the areas such as microdispersions of drugs, cosmetics, paints, and reactions in which the rate is dependent upon the interfacial area since the microemulsions and liquid-crystalline systems offer the maximal surface/volume ratio in oil-water-surfactant systems.

Correspondence concerning this paper should be addressed to D. O. Shah. J. W. Falco is with OSAES, Waterways Experiment Station, U.S. Army Corps of Engineers, Vicksburg, Mississippi 39180.